USING FICTITIOUS TIME INTEGRATION METHOD TO STUDY WAVE PROPAGATION OVER ARBITRARY BATHYMETRY

J.-Y. Chang

Department of Business Administration
Tainan University of Technology
Tainan, Taiwan 71002, R.O.C.

C.-C. Tsai *

Department of Marine Environmental Engineering
National Kaohsiung Marine University
Kaohsiung City, Taiwan 81157, R.O.C.

T.-W. Hsu

Department of Hydraulic and Ocean Engineering
National Cheng Kung University
Tainan, Taiwan 70101, R.O.C.

ABSTRACT

In this study, the fictitious time integration method (FTIM) is applied to investigate wave propagation over an arbitrary bathymetry with measured uncertainty. The FTIM is used to convert the higher-order elliptic mild-slope equation (EMSE) into a FTIM like EMSE (FTIMEMSE). It has the advantage to describe wave transformation from deep water to shallow water region in a large coastal area with numerical efficiency. The validity of the noise resistance for the measured uncertainty of the bathymetry is also studied. In addition, typical examples for waves propagating over an elliptic shoal rest on a horizontal and sloping bottom is presented. It is concluded that the FTIM is robust in the numerical stability and capable of against the noise of the measurement.

Keywords: Fictitious time integration method, Mild slope equation, Water wave.

1. INTRODUCTION

The combined effect of water wave transformations such as shoaling, refraction, diffraction, and reflection can be described by using the mild-slope equation (MSE) that was first derived by Berkhoff [1]. In the derivation of MSE, he assumed a mild slope of the bottom, *i.e.*, $|\nabla_h h|/kh << 1$, and thus neglected the terms of second-order bottom effect proportional to $(\nabla_h h)^2$ and $\nabla_h^2 h$, where $\nabla_h = (\partial/\partial x, \partial/\partial y)$ is the horizontal gradient operator, k is the wave number, and h is the mean water depth. Booij [2] compared the MSE with the finite element model in terms of the reflection coefficient for the case of monochromatic wave propagation over a plane slope. He concluded that the MSE is sufficiently accurate up to a bottom slope of 1:3. The situation where bottom profile is arbitrary and offshore reefs and bars are present on the seabed, the bottom curvature $\nabla_h^2 h$ and possibly higher-orders of the bottom slope-squared $(\nabla_h h)^2$ should be taken into account.

Recently, many studies have attempted to extend the MSE to account for a rapidly varying topography. Kirby [3] extended the mild-slope approximation to include a rapidly varying topography and applied the equation to the reflection of waves passing through the sinusoidal beds. The importance of the higher-order bottom effect terms is in terms of relative water depth based on Chamberlain and Porter's theory (Chamberlain and Porter, [4]). The results were satisfactory for the simulation of wave propagation over the sinusoidal beds. Massel [5] and Chamberlain and Porter [4] used the Galerkin-eigenfunction method to develop an elliptic equation for monochromatic waves. Their results demonstrated the applicability of proposed equations to a rapidly varying topography for which Berkhoff's mild-slope equation failed to produce accurate approximations. Suh *et al*. [6] used Green's second identity and Lagrangian formulation to develop two equivalent hyperbolic equations for wave propagation in a rapidly varying topography. For a monochromatic wave, the model was verified against theoretical and experimental results for the prediction of the reflection coefficients from a plane slope with different inclinations and over a patch of periodic ripples. Following the results of Suh *et al*. [6], Lee *et al*. [7,8] applied the extended mild-slope equations to random wave transformation. Based on Berkhoff's approach, Chandrasekera and Cheung [9] derived an elliptic refraction-diffraction equation that includes the bottom curvature and slope-squared terms. Based on an elliptic

* Corresponding author (tsaichiacheng@mail.nkmu.edu.tw)

DOI : 10.1017/jmech.2013.32
Copyright © 2013 The Society of Theoretical and Applied Mechanics, R.O.C.
https://doi.org/10.1017/jmech.2013.32 Published online by Cambridge University Press

mild-slope equation, Chen *et al*. [10] provided a finite-element model to study the wave–current interaction, where an improved boundary condition (Panchang *et al*., [11]) was considered.

Following the procedure outlined by Copeland [12], Lee *et al*. [13] developed the extended hyperbolic MSE to account for wave transformations over a rapidly varying topography. Their results showed that the hyperbolic equation had the same accuracy as those using the extended elliptic equation.

Following the theoretical approximation of Li [14], Hsu and Wen [15] and Hsu *et al*. [16] extended refraction-diffraction equation to the evolution equation of MSE (EEMSE), in which is converted into a time-dependent parabolic-type equation. The model that includes the higher-order bottom effect terms is extended by Hsu *et al*. [16] to account for a rapidly varying topography and wave energy dissipation in the surf zone. Several computational cases with waves passing through a rapidly varying topography are adopted to test the accuracy of the model. Computational results are also compared with those obtained by existing models. Their model was applied to calculate the problems of wave reflection from a plane slope with different inclinations (Booij, [2]), from a patch of periodic ripples (Davies and Heathershaw, [17]), for the wave height distribution around a circular shoal (Williams *et al*., [18]) and wave breaking on a barred beach (Reniers and Battjes, [19]). The relative importance of the second-order effect terms is also examined in these problems.

Numerical efficiency is the key element of model performance for simulating wave transformations. Consequently, how to get fast convergence speed is of great importance for the treatment of numerical stability. Furthermore, previous studies rarely considered the situation when the measurements of the bathymetry have some noises. However, this case is inevitable since it is very difficult to obtain precise water depth observations in a complicated bottom configuration. In this study, we apply the fictitious time integration method (FTIM) to convert the EMSE (elliptic MSE) into a FTIM like EMSE (FTIMEMSE). In addition, we intend to demonstrate that wave transformations described by FTIMEMSE are not distorted when the measured bathymetries have some noises.

The FTIM was first invented by Liu and Atluri [20] for solving coupled nonlinear algebraic equations based on the Lie-group shooting method (Liu, 21,22). In the FTIM, a fictitious time is introduced to convert the original nonlinear algebraic equations into evolutionary ordinary differential equations. The fixed point of the evolutionary system, which is also the root of the original algebraic equations, is then obtained by applying numerical integrations on the resultant ordinary differential equations, which do not require the derivative of nonlinear algebraic equations. After the development of the FTIM, it was successfully implemented to solve the discretized inverse Sturm-Liouville problems, *m*-point boundary value problems and problems involving Fredholm integral equations by Liu and Atluri [23], Liu [24], and Liu and Atluri [25]. In all of these applications, the problems were first discretized into nonlinear algebraic equations and then formally solved by the FTIM.

In addition to nonlinear algebraic equations, Liu and Atluri [26] introduced the application of the FTIM to solve a nonlinear optimization problem (NOP) under multiple equality and inequality constraints. The Kuhn-Tucker optimality conditions were used to transform the NOP into a mixed complementary problem. Meanwhile, the FTIM has been adopted to tackle two-dimensional nonlinear elliptic boundary value problems by Liu [27] and Liu [28]. In order to improve the efficiency, Ku *et al*. [29] improved the FTIM by introducing a new time-like function to solve nonlinear PDEs.

In addition, the FTIM have been adopted in several practical applications. For example, direct heat conduction problem (DHCP) and backward heat conduction problem (BHCP) were numerically solved by a parabolic type evolution equation reformed through the FTIM. Also, Chang [30] proposed a FTIM model for solving the nonhomogeneous backward heat conduction (BHCPs) and multi-dimensional nonlinear problems. Afterward, a new FTIM model was proposed for studying the multi-dimensional backward wave problems (BWPs) by Chang [31].

Following the researches mentioned above, the FTIM was found to be robust against the noise when it is used to solve many problems involving the Fredholm integral equations. With the aid of this attribute, the FTIM is employed in the present study to develop a FTIM from EMSE (FTIMEMSE), and investigate wave transformations over an arbitrary bathymetry with measured uncertainties. Our numerical results indicate that the method is more robust than the direct solution of the EMSE. Moreover, the CPU time and the number of iteration of present model are less than the EMSE in calculating same cases. Overall, numerical results showed that the application of the FTIM on the EMSE can simulate wave propagation reasonably for not only a large number of grid nodes but also noise resistance. This result concludes that it is very suitable for practical problems.

2. THE FTIM INCORPORATE WITH EMSE (FTIMEMSE)

The EMSE is commonly used for describing wave transformations from an offshore to nearshore region in a large coastal region and is written in the form

$$\nabla_h \cdot (CC_g \nabla_h \phi) + k^2 CC_g (1 + if_D)\,\phi + \left[f_1(kh) g \nabla_h{}^2 h + f_2(kh)(\nabla_h h)^2 gk \right] \phi = 0 \qquad (1)$$

where $\phi(x, y)$ is the complex velocity potential, f_D is the combined energy coefficient including the nonlinear shoaling factor and energy dissipation factor, C is the wave celerity, C_g is the group velocity, g is the gravitational acceleration, f_1 and f_2 are the coefficients of the bottom curvature and bottom slop-squared terms, respectively. The expressions of f_1, f_2 and f_D are referred

https://doi.org/10.1017/jmech.2013.32 Published online by Cambridge University Press

to Hsu and Wen [15]. Following Radder [32], a scale factor of the velocity potential expressed as

$$\varphi = \sqrt{CC_g}\,\phi \tag{2}$$

is introduced into Eq. (1) and the mathematical manipulation yields the Helmholtz equation:

$$\nabla_h^2\varphi + k_c^2\varphi = 0 \tag{3}$$

where k_c is a pseudo wavenumber given by

$$k_c^2 = k^2(1+if_D) - \frac{\nabla_h{}^2\sqrt{CC_g}}{\sqrt{CC_g}} + \frac{\left[f_1 g\nabla_h{}^2 h + f_2(\nabla_h h)^2 gk\right]}{CC_g} \tag{4}$$

To apply the FTIM in the EMSE, we introduce a function $w(x, y, t)$ defined by

$$w(x,\ y,\ t) = \varphi(x,\ y)\ q(t) \tag{5}$$

where t is a fictitious time and $q(t)$ is the FTIM time-like function. The velocity potential is thus in terms of

$$\varphi(x,\ y) = \frac{w(x,\ y,\ t)}{q(t)} \tag{6}$$

Taking the partial derivative of Eq. (5) with respect to t, we have

$$\frac{\partial w}{\partial t} = \varphi\frac{dq}{dt} \tag{7}$$

Then we multiply Eq. (3) by a non-zero coefficient, v, leading to the following result,

$$\nu[\nabla_h^2\varphi + k_c^2\varphi] = 0 \tag{8}$$

Adding Eqs. (7) and (8), we have

$$\frac{\partial w}{\partial t} + \nu[\nabla_h^2\varphi + k_c^2\varphi] = \varphi\frac{dq}{dt} \tag{9}$$

Making use of Eq. (6), we obtain

$$\frac{\partial w}{\partial t} + \nu[\nabla_h^2\varphi + k_c^2\varphi] = \frac{w}{q}\frac{dq}{dt} \tag{10}$$

Equation (10) is further expressed by

$$\frac{1}{q}\frac{\partial w}{\partial t} + \frac{\nu}{q}[\nabla_h^2\varphi + k_c^2\varphi] = \frac{w}{q^2}\frac{dq}{dt} \tag{11}$$

By using the following partial derivative

$$\frac{\partial}{\partial t}\left(\frac{w}{q}\right) = \frac{1}{q}\frac{\partial w}{\partial t} - \frac{w}{q^2}\frac{dq}{dt} \tag{12}$$

and inserting Eqs. (6) and (12) into Eq. (11), the resultant equation reads

$$\frac{\partial\varphi}{\partial t} + \frac{\nu}{q}[\nabla_h^2\varphi + k_c^2\varphi] = 0 \tag{13}$$

Following Liu and Atluri [23] and Ku *et al*. [29], we use the following time-like function to convert Eq. (13), which is written in the from

$$q(t) = (1+t)^M \tag{14}$$

where M is a parameter to accelerate the convergence of the FTIM.

We notice that Eq. (13) becomes a diffusion equation for $v = \pm 1$, and is equivalent to the EEMSE of Li [14] for the case of $v = (2i\omega)^{-1}$ and $q = 1$, where ω is the angular frequency. From physical point of view, v is specified to account for the damping coefficient, and $q(t)$ is the time-like function to increase the convergence speed of numerical computation.

3. BOUNDARY CONDITION

The radiation boundary conditions (RBC) in the MSE are specified so that waves are forced to go out radically along the bounder of a computational domain. According to Hsu and Wen [15], there are three types of RBC: A full or partial reflection radiation boundary condition and a given boundary condition which are specified along the boundary of x and y directions, respectively, as follows.

$$\varphi_x = \pm(-1)^m i\alpha\varphi k\cos\theta + 2i\varphi_i\, k\cos\theta \tag{15}$$

$$\varphi_y = \pm(-1)^m i\alpha\varphi k\sin\theta + 2i\varphi_i\, k\sin\theta \tag{16}$$

where $\alpha = (1 - R)/(1 + R)$ is an absorption coefficient; R is a reflection coefficient, θ is the approaching wave angle to the boundary; and φ_i denotes a given velocity potential at the boundary of incident waves. For full reflection, $\varphi_i = 0$, $m = 0$, and $\alpha = 0$; for partial reflection, $\varphi_i = 0$, $m = 0$, and $0 < \alpha \le 1$; and for a given boundary condition, $m = 1$ and $\alpha = 1$. The incident velocity potential is given by linear wave theory, that is

$$\varphi_i = (igH_i\sqrt{CC_g}/2\omega)\cos\left(\begin{matrix}k_0\, x\cos\theta_0 + \\ k_0\, y\sin\theta_0 - \omega t\end{matrix}\right) \tag{17}$$

in which H_i is a monochromatic incident wave height and θ_0 is the wave angle for the incident wave.

In this study, an improved radiation boundary condition proposed by Hsu *et al*. [33] for the cross-shore open boundaries with an irregular bathymetry is proposed in this study. The total wave velocity, φ, are decomposed into the incident wave velocity φ_i, the outgoing scattering wave velocity φ_s, and the reflected wave velocity φ_r, *i.e.* $\varphi = \varphi_i + \varphi_r + \varphi_s$. It is desirable to define $\varphi_0 = \varphi_i + \varphi_r$ for separating the scattering waves in the calculation. Due to the varying topography, the value of φ_0 along the cross-shore open boundaries is unknown and needed to be estimated initially by the method of Panchang *et al*. [11]. For this reason,

https://doi.org/10.1017/jmech.2013.32 Published online by Cambridge University Press

we use the wave model developed by Hsu *et al*. [34] to solve φ_0. Therefore, the improved radiation boundary condition along the boundary of y direction which are on the lateral computing domain could be rewritten as

$$\varphi_y = \pm(-1)^m i\alpha\varphi k\sin\theta + \varphi_{0y} - i\alpha\varphi_0 k\sin\theta \qquad (18)$$

By using Eq. (18), initial boundary conditions can be reasonable calculated. It is noted that a general type of RBC for arbitrarily chosen open boundaries is proposed in the present model. Additionally, details can be referred Hsu *et al*. [34].

In addition, the computing process of present model is illustrated as following. First of all, we obtain the input data such as wave and bathymetry information from statistical, experimental, or observing consequences. Then, the values of φ_0, one of the most important parts in the improved radiation boundary condition, can be computed by the model of Hsu *et al*. [34]. Afterwards, the present model can be applied for obtaining the transformed wave field.

4. VERIFICATIONS

The developed new type of the FTIMEMSE model was derived using FTIM to incorporate the EMSE for simulating wave propagation over arbitrary bathymetries or coastal structures. For the proposed model laboratory experiments and field surreys have been carried out to obtain estimates of the performance of the comparison. In this study, two typical cases of wave propagating were used to test the model. The ability of the noise resistance is investigated for the condition of uncertainly measured bathymetry.

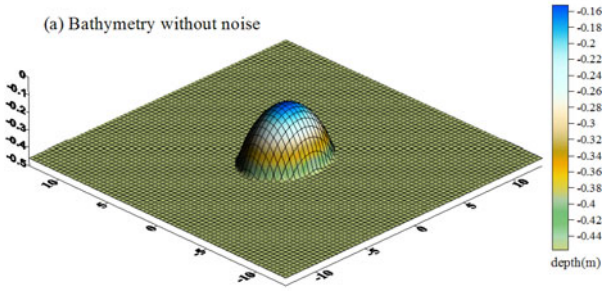
4.1 Case1: The Elliptic Shoal Rest on a Flat Bottom

The elliptic shoal rest on the bottom of a laboratory wave tank has major and minor radii of 3.96m and 3.05m, respectively. The experiment was conducted by Vincent and Briggs [35] for wave travelling across the shoal, with significant refraction-diffraction effect and caustics behind the shoal. The water depth of the elliptic shoal topography is given by

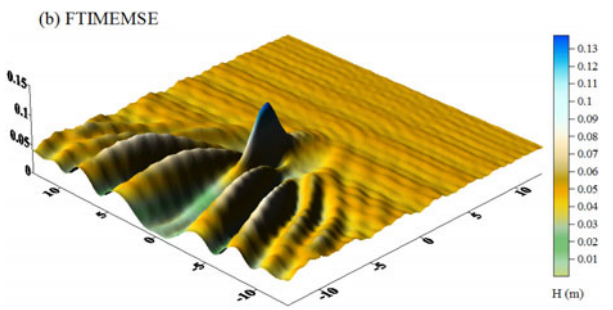
$$h(x,\ y) = 0.9144 - 0.762\sqrt{1 - \frac{x^2}{(4.95)^2} - \frac{y^2}{(3.81)^2}}\ ,$$
$$\frac{x^2}{(3.96)^2} + \frac{y^2}{(3.05)^2} \le 1$$
$$h(x,\ y) = 0.457\ ,\quad \frac{x^2}{(3.96)^2} + \frac{y^2}{(3.05)^2} > 1 \qquad (19)$$

The geometry can be seen in Fig. 1(a). The incident wave with a period of $T = 1.3$sec and $H_i = 0.0464$m are normal to the offshore boundary. The numerical simulation was run in a computational domain of 261 × 261 grid nodes with a time step $\Delta t = 0.01$sec and a grid space $\Delta x = \Delta y = 0.1$m, respectively.

The computed wave height pattern with measured noise is presented in Fig. 1(b). It can be seen that a strong wave focus is formed behind the elliptic shoal. We note that a new parameter M is introduced to the time-like function for manipulating the speed of convergence. A numerical test was also conducted using the time-like function to solve Eq. (13) by setting $v = 1.0$ and M is varying from $M = 0$ to $M = 1$. Figure 2 demonstrates the comparison between the error and the fictitious time step with different values of M, where the error is defined as the absolute value of the difference between calculated solution and measurements. From Fig. 2, it is found that the parameter M in the new time-like function clearly increases the convergence speed. The present results showed that smaller values of M produce, the faster convergence speed except for $M = 0$, in which $q(t)$ is not a time-like function and become a constant.



(a) Bathymetry



(b) Wave patterns

Fig. 1 Results of wave patterns for the bathymetry without noise

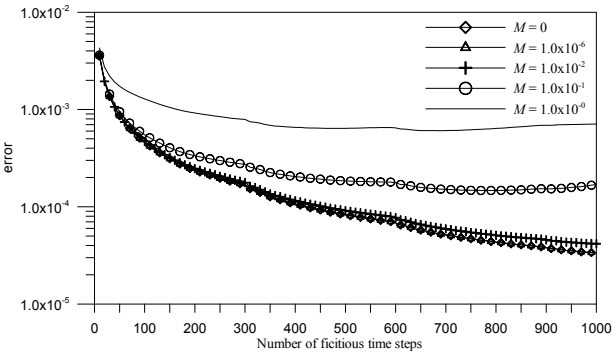


Fig. 2 Comparison of error for different values of M (bathymetry without noise)

https://doi.org/10.1017/jmech.2013.32 Published online by Cambridge University Press

As the wave field usually depends on the geometry as well as bottom configuration, the accurate surveying of the coastal topography provides much valuable information on the spatial and temporal behavior of wave motion. Some of the difficult problems in a coastal survey are the measurement of bathymetry in the surf zone and tidal flat. The uncertainty of the survey or the noise of measurement is unavoidable when we detect a realistic water depth. To show model's performance in resisting the noise in the numerical simulation, wave height predictions over an area with noise were tested.

Iso-wave amplitude lines are show in Fig. 3, in which Fig. 3(a) shows the bathymetry having a 2.5% random noise. Figure 3(b) presents the wave patterns predicted by EMSE without the help of FTIM. Figure 3(c) depicts the computed wave field using of Hsu *et al*. [33] FTIMEMSE. It is evident that the present model obtains a good performance against the noise resulting from bathymetric survey. In order to show that the FTIMEMSE plays an important role in noise resistance, a computation using a random noise of 10% for the same condition presents the results in Fig. 4.

The ability of resisting noise in the computation is evaluated based on the relative error defined by

$$Er(\%) = \frac{\sum_{i=1}^{nx}\sum_{j=1}^{ny}\left(\frac{|H_{i,j} - H_{i,j}^{*}|}{H_{i,j}}\right)}{nx \times ny} \tag{20}$$

where Er is a relative error, $H_{i,j}$ is the computed wave height when water depth has no measured uncertainty; and $H_{i,j}^{*}$ is the calculated wave when the bathymetry has the noise. The comparison of the relative errors using FTIMEMSE and EMSE developed by Hsu *et al*. [33] is presented in Table 1. We notice that the FTIMEMSE model givens better results for resisting errors of different random noises. Furthermore, a comparison of the computing time between the FTIMEMSE and EMSE is shown in Table 2. It is clear that the computing time of the FTIMEMSE is much less than that of the EMSE especially in the cases of higher random noise. Note that the computing time is slightly growing with the increase of random noise in the FTIMEMSE model. Nevertheless, it is rapidly growing in the EMSE model mainly because the bathymetry with higher random noise leads the convergence process to be unstable. Accordingly, the results show that the present model is more efficient than the previous EMSE model for resisting noise indeed.

4.2 Case2: The Elliptic Shoal Located on a Sloping Beach

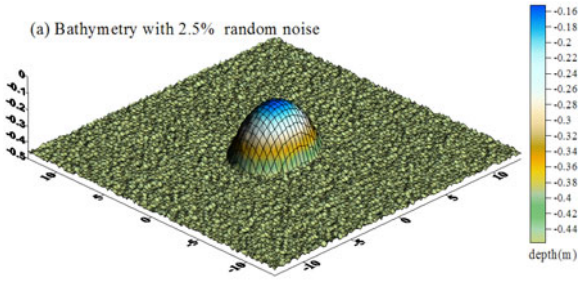
The FTIMEMSE model is further applied to the test case of Brekhoff [1]. The elliptic shoal located on a sloping beach and the geometry is presented in Fig. 5(a). The slope-oriented coordinates (x', y') related to the computational coordinates (x, y) is given by

Table 1 Comparisons of the relative error *Er* using FTIMEMSE and EMSE

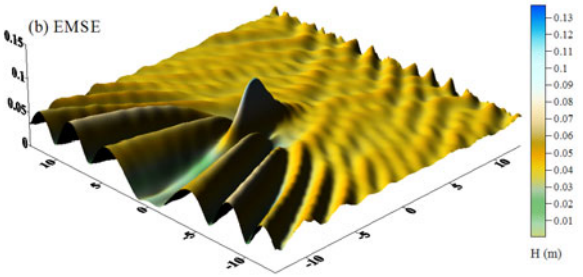
Models \ *Er*	*Er* (noise = 2.5%)	*Er* (noise = 10.0%)
FTIMEMSE (Case1)	2.26%	6.84%
EMSE (Case1)	4.16%	22.90%
FTIMEMSE (Case2)	2.41%	4.04%

Table 2 Comparisons of elapsed time (s) between the FTIMEMSE and EMSE in Case 1

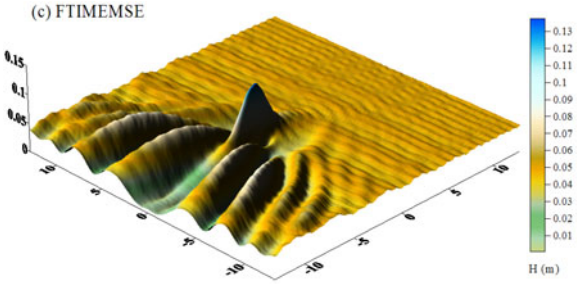
Case \ Models	FTIMEMSE	EMSE
Bathymetry with a random noise of 2.5%	164sec	344sec
Bathymetry with a random noise of 10.0%	209sec	2673sec



(a) Bathymetry



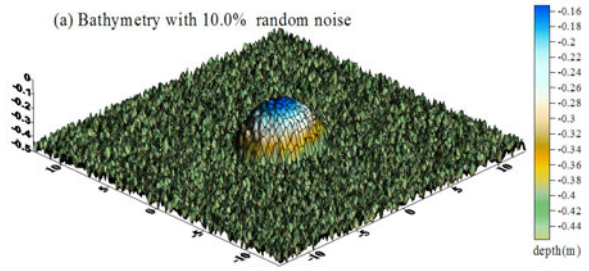
(b) Wave patterns (using Eq. (1), EMSE)



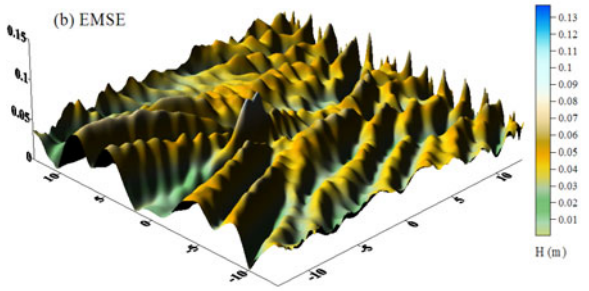
(c) Wave patterns (using Eq. (13), FTIMEMSE)

Fig. 3 Results of wave patterns for the bathymetry with a random noise of 2.5%

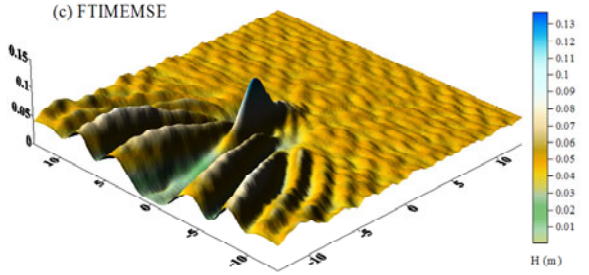
https://doi.org/10.1017/jmech.2013.32 Published online by Cambridge University Press



(a) Bathymetry

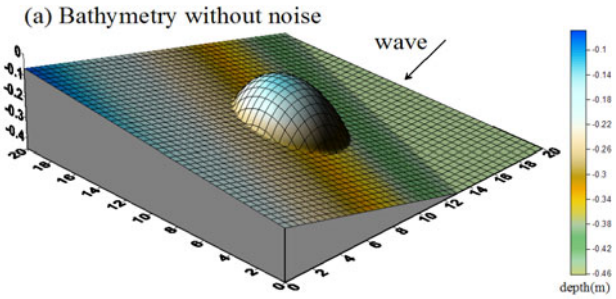


(b) Wave patterns (using Eq. (1), EMSE)

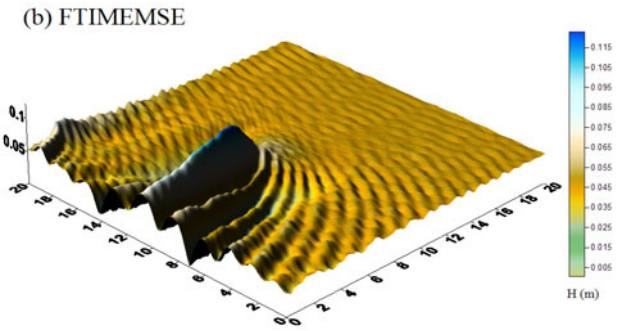


(c) Wave patterns (using Eq. (13), FTIMEMSE)

Fig. 4 Results of wave patterns for the bathymetry with a random noise of 10%



(a) Bathymetry



(b) Wave patterns

Fig. 5 Results of wave patterns for the bathymetry without noise

$$\begin{aligned} x' &= (x-10.5)\cos 20^\circ - (y-10)\sin 20^\circ \\ y' &= (y-10)\cos 20^\circ + (x-10.5)\sin 20^\circ \end{aligned} \tag{21}$$

where (10.5, 10) is the centre of the shoal. The water depth on the slope is described by

$$\begin{cases} h_s = 0.45 - 0.02\cdot(15.84 - x_s) & \text{for } x_s < 15.84 \\ h_s = 0.45 & \text{for } x_s \geq 15.84 \end{cases} \tag{22}$$

where the coordinate x_s is oriented from the centre of the shoal. The water depth is redefined as

$$\begin{cases} h = h_s + 0.3 - 0.5\cdot\sqrt{1-\left(\dfrac{x'-10.5}{3.75}\right)^2 - \left(\dfrac{y'-10}{5}\right)^2} \\ \qquad \text{for } \left(\dfrac{x'-10.5}{3}\right)^2 + \left(\dfrac{y'-10}{4}\right) < 1 \\ h = h_s \\ \qquad \text{for } \left(\dfrac{x'-10.5}{3}\right)^2 + \left(\dfrac{y'-10}{4}\right) \geq 1 \end{cases} \tag{23}$$

The FTIMEMSE was run on a numerical domain of 401 × 401 nodes with $\Delta x = \Delta y = 0.05$m and $\Delta t = 0.01$sec on the computation domain of 20.0m × 20.0m. The incident wave condition is $H_i = 0.0464$m and $T = 1.0$sec, respectively.

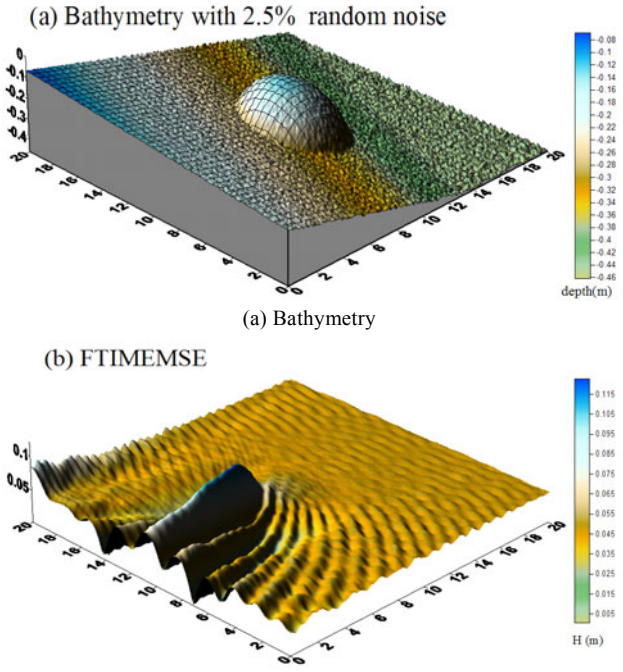
The wave pattern computed from the present model for the bathymetry without noise is presented in Fig. 5(a). The results of the present model show that a caustics is remarkable behind the elliptic shoal. Note that the present model predicts a sub tantial wave height distrition due to wave refraction, diffraction and reflection.

Two typical cases with randomnoises of 2.5% and 10% were tested to explore the ability of FTIMEMSE against the bathymetry uncertainty. The computed wave height patterns are demostated in Figs. 6 and 7 for the two cases, respectively. It can be seen in both figures that the present model is capable of decreasing measured noises in the numerical simulation. And the relative error is also presented in Table 1. It is shown that the FTIMEMSE model is capable of against the noise of the measurement.

5. CONCLUSIONS

The fictitious time integration method (FTIM) proposed by Liu and Atluri [20] is employed to investigate wave propagation over an arbitrary bathymetry with measured noise. The FTIM is used to convert the higher-order elliptic mild-slop equation (EMSE) into a FTIM like EMSE (FTIMEMSE). The equation is equivalent to the formal evolution equation of mild slop equation (EEMSE) if the time like function is set to be a constant. It has the advantage to simulate wave transformation from an offshore region to a nearshore region including wave breaking and energy dissipation in a large coastal area with numerical efficiency.

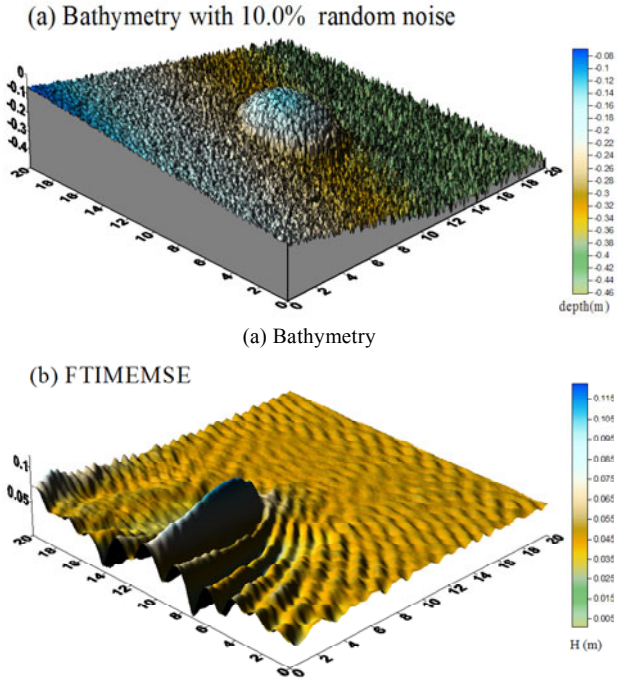
https://doi.org/10.1017/jmech.2013.32 Published online by Cambridge University Press



(a) Bathymetry

(b) Wave patterns

Fig. 6 Results of wave patterns for the bathymetry with a random noise of 2.5%



(a) Bathymetry

(b) Wave patterns

Fig. 7 Results of wave patterns for the bathymetry with a random noise of 10%

Friendly speaking, the usefulness of FTIMEMSE in describing wave propagation has been demonstrated for the test case of an elliptic shoal located on a sloping bottom. The present model has been shown to be very efficient and with less iteration than the previous EMSE model to achieve a fast convergence speed to find the solution.

For the case where the bathymetry is measured with uncertainty, the FTIMEMSE can be done fairly efficiently with the help of the time-like function. The numerical results showed that the model is capable of reducing the errors in numerical calculation for the cases of random noises are exited. Furthermore, the model has a flexible form, which is helpful to adjust the coefficient of the time-like function for accelerating the convergence rate with economical cost in practical applications.

ACKNOWLEDGMENTS

This research is supported by the National Science council under Grant No. NSC 101-3113-P-006-015, Taiwan. It is also sponsored by the Ministry of Education, Taiwan, R.O.C. under the NCKU Project of Promoting Academic Excellence & Developing World Class Research Centers

REFERENCES

1. Berkhoff, J. C. W., "Computation of Combined Refraction-Diffraction," *13th International Conference on Coastal Engineering*, pp. 471–490 (1972).
2. Booij, N., "A Note on the Accuracy of the Mild-Slope Equation," *Coastal Engineering*, **7**, pp. 191–203 (1983).
3. Kirby, J. T., "Higher-Order Approximations in the Parabolic Equation Method for Water Waves," *Journal of Geopphysical Research*, **91**, pp. 933–952 (1986).
4. Chamberlain, P. G. and Porter, D., "The Modified Mild-Slope Equation," *Journal of Fluid Mechanics*, **291**, pp. 393–407 (1995).
5. Massel, S. R., "Extended Refraction-Diffraction Equation for Surface Waves," *Coastal Engineering*, **19**, pp. 97–126 (1993).
6. Suh, K. D., Lee, C. and Park, W. S., "Time-Dependent Equations for Wave Propagation on Rapidly Varying Topography," *Coastal Engineering*, **32**, pp. 91–117 (1997).
7. Lee, C., Kim, G. and Suh, K. D., "Extended Mild-Slope Equation for Random Waves," *Coastal Engineering*, **48**, pp. 277–287 (2003).
8. Lee, C., Kim, G. and Suh, K. D., "Comparison of Time-Dependent Extended Mild-Slope Equations for Random Waves," *Ocean Engineering*, **53**, pp. 311–318 (2006).
9. Chandrasekera, C. N. and Cheung, K. F., "Extended Linear Refraction-Diffraction Model," *Journal of Waterway, Port, Coastal, and Ocean Engineering*, **123**, pp. 280–286 (1997).
10. Chen, W., Panchang, V. and Demirbilek, Z., "On the Modeling of Wave–Current Interaction Using the Elliptic Mild-Slope Wave Equation," *Ocean Engineering*, **32**, pp. 2135–2164 (2005).

https://doi.org/10.1017/jmech.2013.32 Published online by Cambridge University Press

11. Panchang, V., Chen, W., Xu, B., Schlenker, K., Demirbilek, Z. and Okihiro, M., "Exterior Bathymetric Effects in Elliptic Harbor Wave Models," *Journal of Waterway, Port, Coastal, and Ocean Engineering*, **126**, pp. 71–78 (2000).
12. Copeland, G. J. M., "A Practical Alternative to the "Mild-Slope" Wave Equation," Coastal Engineering, **9**, pp. 125–149 (1985).
13. Lee, C., Sun Park, W., Cho, Y.-S. and Doug Suh, K., "Hyperbolic Mild-Slope Equations Extended to Account for Rapidly Varying Topography," *Coastal Engineering*, **34**, pp. 243–257 (1998).
14. Li, B., "An Evolution Equation for Water Waves," *Coastal Engineering*, **23**, pp. 227–242 (1994).
15. Hsu, T.-W. and Wen, C.-C., "A Parabolic Equation Extended to Account for Rapidly Varying Topography," *Ocean Engineering*, **28**, pp. 1479–1498 (2001).
16. Hsu, T.-W., Lin, T.-Y., Wen, C.-C. and Ou, S.-H., "A Complementary Mild-Slope Equation Derived Using Higher-Order Depth Function for Waves Obliquely Propagating on Sloping Bottom," *Physics of Fluids*, **18**, http://dx.doi.org/10.1063/1.2337734 (2006).
17. Davies, A. G. and Heathershaw, A. D., "Surface-Wave Propagation over Sinusoidally Varying Topography," *Journal of Fluid Mechanics*, **144**, pp.419–443 (1984).
18. Williams, R. G., Darbyshire, J., Holmes, P. and Berkhoff, J. C. W., "Wave Refraction and Diffraction in a Caustic Region: A Numerical Solution and Experimental Validation," *ICE Proceedings*, **69**, pp. 635–649 (1980).
19. Reniers, A. J. H. M. and Battjes, J. A., "A Laboratory Study of Longshore Currents over Barred and Non-Barred Beaches," *Coastal Engineering*, **30**, pp. 1–21 (1997).
20. Liu, C. S. and Atluri, S. N., "A Novel Time Integration Method for Solving a Large System of Non-Linear Algebraic Equations," *Computer Modeling in Engineering & Sciences*, **31**, pp. 71–84 (2008).
21. Liu, C. S., "A Lie-Group Shooting Method for Simultaneously Estimating the Time-Dependent Damping and Stiffness Coefficients," *Computer Modeling in Engineering & Sciences*, **27**, pp. 137–150 (2008).
22. Liu, C. S., "The Lie-Group Shooting Method for Nonlinear Two-Point Boundary Value Problems Exhibiting Multiple Solutions," *Computer Modeling in Engineering & Sciences*, **5**, pp. 55–84 (2008).
23. Liu, C. S. and Atluri, S. N., "A Novel Fictitious Time Integration Method for Solving the Discretized Inverse Sturm-Liouville Problems, for Specified Eigenvalues," *Computer Modeling in Engineering & Sciences*, **36**, pp. 261–285 (2008).
24. Liu, C. S., "A Fictitious Time Integration Method for Solving M-Point Boundary Value Problems," *Computer Modeling in Engineering & Sciences*, **39**, pp. 125–154 (2009).
25. Liu, C. S. and Atluri, S. N., "A Fictitious Time Integration Method for the Numerical Solution of the Fredholm Integral Equation and for Numerical Differentiation of Noisy Data, and Its Relation to the Filter Theory," *Computer Modeling in Engineering & Sciences*, **41**, pp. 243–261 (2009).
26. Liu, C. S. and Atluri, S. N., "A Fictitious Time Integration Method (FTIM) for Solving Mixed Complementarity Problems with Applications to Non-Linear Optimization," *Computer Modeling in Engineering & Sciences*, **34**, pp. 155–178 (2008).
27. Liu, C. S., "A Fictitious Time Integration Method for Two-Dimensional Quasilinear Elliptic Boundary Value Problems," *Computer Modeling in Engineering & Sciences*, **33**, pp. 179–198 (2008).
28. Liu, C. S., "A Fictitious Time Integration Method for a Quasilinear Elliptic Boundary Value Problem, Defined in an Arbitrary Plane Domain," *Computers Materials & Continua*, **11**, pp. 15–32 (2009).
29. Ku, C. Y., Yeih, W. C., Liu, C. S. and Chi, C. C., "Applications of the Fictitious Time Integration Method Using a New Time-Like Function," *Computer Modeling in Engineering & Sciences*, **43**, pp. 173–190 (2009).
30. Chang, C. W., "A Fictitious Time Integration Method for Multi-Dimensionalbackward Heat Conduction Problems," *Computers, Materials & Continua*, **19**, pp. 285–314 (2010).
31. Chang, C. W., "A Fictitious Time Integration Method for Multi-Dimensional Backward Wave Problems," *Computers, Materials & Continua*, **21**, pp. 87–105 (2011).
32. Radder, A. C., "On the Parabolic Equation Method for Water-Wave Propagation," *Journal of Fluid Mechanics*, **95**, pp. 159–176 (1979).
33. Hsu, T.-W., Lan, Y.-J., Wang, Y.-H. and Tsai, C.-Y., "Using Finite-Element Method to Simulate Wave Transformations in Surf Zone," *Journal of Engineering Mechanics*, **131**, pp. 1214–1217 (2005).
34. Hsu, T.-W., Chang, J.-Y., Lan, Y.-J., Lai, J.-W. and Ou, S.-H., "A Parabolic Equation for Wave Propagation over Porous Structures," *Coastal Engineering*, **55**, pp. 1148–1158 (2008).
35. Vincent, C. L. and Briggs, M. J., "Refraction-Diffraction of Irregular Waves over a Mound," *Journal of Waterway, Port, Coastal, and Ocean Engineering*, **115**, pp. 269–284 (1989).

(Manuscript received May 17, 2011,
accepted for publication February 18, 2013.)

https://doi.org/10.1017/jmech.2013.32 Published online by Cambridge University Press